

A robust approach to warped Gaussian process-constrained optimization

Johannes Wiebe¹, Inês Cecílio², Jonathan Dunlop², and Ruth Misener¹

¹Department of Computing, Imperial College London, London, UK

²Schlumberger Cambridge Research, Cambridge, UK

Abstract

Optimization problems with uncertain black-box constraints, modeled by warped Gaussian processes, have recently been considered in the Bayesian optimization setting. This work introduces a new class of constraints in which the same black-box function occurs multiple times evaluated at different domain points. Such constraints are important in applications where, e.g., safety-critical measures are aggregated over multiple time periods. Our approach, which uses robust optimization, reformulates these uncertain constraints into deterministic constraints guaranteed to be satisfied with a specified probability, i.e., deterministic approximations to a chance constraint. This approach extends robust optimization methods from parametric uncertainty to uncertain functions modeled by warped Gaussian processes. We analyze convexity conditions and propose a custom global optimization strategy for non-convex cases. A case study derived from production planning and an industrially relevant example from oil well drilling show that the approach effectively mitigates uncertainty in the learned curves. For the drill scheduling example, we develop a custom strategy for globally optimizing integer decisions.

1 Introduction

In mathematical programming, optimization under uncertainty often focuses on parametric uncertainty [10, 13, 16, 51, 56]. But many application areas rely on uncertain,

expensive to evaluate black-box functions, e.g., automatic chemical design, production planning, scheduling with equipment degradation, adaptive vehicle routing, automatic control and robotics, and biological systems [15, 21, 23, 29, 36, 57, 60].

Bayesian optimization optimizes such functions by (i) fitting a Gaussian process to a small number of collected data points and (ii) subsequently choosing new sampling points using an acquisition function [41, 53, 55]. The Bayesian optimization literature also considers problems with black-box constraints, e.g., by multiplying the acquisition function with the probability of constraint satisfaction [25, 26, 47]. The global optimization community often handles black-box constraints by (i) generating a small data set from the black box function, (ii) fitting a surrogate model to this data, and (iii) replacing the black box constraint by the surrogate model [14, 18, 19, 30, 39, 42, 50]. This approach, however, rarely considers uncertainty in the black box function.

One way of including uncertain black-box function into the optimization problem is to consider the surrogate model’s parameters to be uncertain and use classical parametric uncertainty methods. Hüllen et al. [33] recently demonstrated this approach for polynomial surrogates using robust optimization. This paper proposes a more direct approach utilizing probabilistic surrogate models to model the uncertain curves. We study optimization problems with constraints which aggregate black-box functions:

$$\sum_i \tilde{a}_i x_i \leq b \tag{1a}$$

$$\tilde{a}_i = g(\mathbf{y}_i), \tag{1b}$$

where x_i is a decision variable and \tilde{a}_i depends on a vector of decision variables $\mathbf{y}_i \in \mathbb{R}^k$ through a black-box function $g(\cdot)$. Constraint (1) occurs in many highly relevant applications. In production planning, one may limit the total allowed equipment degradation $\sum_i r(p_i)\Delta t_i \leq b$, where $r(p_i)$ is the black-box degradation rate depending on production p_i in time period i and Δt_i is equipment operation time in period i [60]. A second example is vehicle routing, where the total traveling time $\sum_i \Delta t(t_i, s_i, d_i)\gamma_i$ is the sum of traveling times $\Delta t(t_i, s_i, d_i)$ for individual legs i , dependent on starting time t_i , source s_i , and destination d_i , and γ_i is a binary variable indicating whether leg i is part of the route. A third example is project scheduling under uncertainty in which duration uncertainty may be aggregated over multiple activities [58]. Lastly, the drill scheduling case study described in detail later in this paper is an industrially relevant example.

When black-box constraints are risk or safety-critical, hedging solutions against uncertainty is essential. Evaluating black-box functions may require expensive com-

puter simulations or physical experiments, so available data is generally limited and may be subject to model errors and measurement noise. We therefore consider the function $g(\cdot)$ to be uncertain and aim to find solutions for which Constraint (1) holds with confidence $1 - \alpha$:

$$P\left(\sum_i g(\mathbf{y}_i)x_i \leq b\right) \geq 1 - \alpha. \quad (2)$$

To capture the uncertainty in $g(\cdot)$, we model it by stochastic surrogate models. A common stochastic surrogate is the Gaussian process (GP) model. Depending on the underlying data generating distribution, however, a GP may be an inadequate model. Warped Gaussian processes, which map observations to a latent space using a warping function, are an alternative, more flexible model [54]. This paper considers both standard and warped GPs.

We note that other contributions have connected Bayesian optimization with robust optimization [7, 11, 12, 17]. In this setting, an adversary can perturb the input \mathbf{x} by $\boldsymbol{\delta} \in \mathcal{U}$. Robust solutions optimize performance under the worst-case perturbation realization: $\min_{\mathbf{x} \in \mathbb{R}^n} \max_{\boldsymbol{\delta} \in \mathcal{U}} f(\mathbf{x} + \boldsymbol{\delta})$.

Contributions. For the standard GP model, we show how chance constraint Eq. (2) can be exactly reformulated as a deterministic constraint using existing approaches. For the warped case, we develop a robust optimization approach which conservatively approximates the chance constraint. By constructing decision-dependent uncertainty sets from confidence ellipsoids based on the warped GP models, we obtain probabilistic constraint violation bounds. We utilize Wolfe duality to reformulate the resulting robust optimization problem and obtain explicit deterministic robust counterparts. This reformulation expresses uncertain constraints, modeled by GPs, as deterministic constraints with a guaranteed probability of constraint satisfaction, i.e., deterministic approximations to a chance constraint. We analyze convexity conditions of the warping function under which the Wolfe duality based reformulation is applicable. For non-convex cases, we develop a global optimization strategy which utilizes problem structure. To reduce solution conservatism, we furthermore propose an iterative a posteriori procedure of selecting the uncertainty set size which complements the obtained a priori guarantee.

We show how the proposed approach hedges against uncertainty in learned curves for two case studies: i) a production planning-inspired case study with an uncertain price-supply curve and ii) an industrially relevant drill-scheduling case study with uncertain motor degradation characteristics. For the drill-scheduling case study we develop a custom strategy for dealing with discrete decisions.

Notation. See Appendix A for a table of notation.

2 Method

Sections 2.1-2.3 review (warped) GPs, robust optimization, and chance constraint reformulations for Gaussian distributions. Sections 2.4 and 2.5 outline our proposed robust approximation approach.

2.1 Warped Gaussian processes

GPs are widely used for Bayesian optimization and non-parametric regression [49, 53, 61].

Definition 1 (Gaussian process). *A continuous stochastic process $G(\mathbf{x})$ for which $G_{\mathbf{x}_1, \dots, \mathbf{x}_l} = (G_{\mathbf{x}_1}, \dots, G_{\mathbf{x}_l})$ is a multivariate Gaussian random variable for every finite set of points $\mathbf{x}_1, \dots, \mathbf{x}_l$.*

A GP defines a probability distribution over functions and it is fully specified by its mean function $m(\cdot)$ and kernel function $k(\cdot, \cdot)$. Given a set of N data points $X = [\mathbf{x}_1, \dots, \mathbf{x}_N]$, $\mathbf{y} = [y_1, \dots, y_N]^\top$ and using a zero mean function, we can predict the mean $\boldsymbol{\mu}$ and covariance matrix Σ of the multivariate Gaussian distribution defined by a set of new test points $X_* = [\mathbf{x}_1^*, \dots, \mathbf{x}_n^*]$:

$$\begin{aligned}\boldsymbol{\mu}(X_*) &= K(X_*, X)[K(X, X) + \sigma_n^2 I]^{-1} \mathbf{y} \\ \Sigma(X_*) &= K(X_*, X_*) \\ &\quad - K(X_*, X)[K(X, X) + \sigma_n^2 I]^{-1} K(X, X_*),\end{aligned}$$

where σ_n is the standard deviation of noise in the data, $K(X_*, X) = K(X, X_*)^\top$ is the $n \times N$ covariance matrix between test and training points, $K(X, X)$ the $N \times N$ covariance matrix between training points, $K(X_*, X_*)$ the $n \times n$ covariance matrix between test points, and I the identity matrix. We denote the ij -element of Σ as $\sigma_{ij}^2 = \sigma^2(\mathbf{x}_i^*, \mathbf{x}_j^*)$.

The standard GP approach assumes that the data follows a multivariate Gaussian. While this assumption allows prediction using simple matrix multiplication, it can be unreasonable for non-Gaussian data [54]. A slightly more flexible model, which still retains many of the benefits of GPs, is the warped GP model. The key idea is to warp the observations \mathbf{y} to a latent space ξ using a monotonic warping function $\xi = h(\mathbf{y}, \Psi)$. A standard GP then models the data in the latent space $\xi \sim \mathcal{GP}(\mathbf{x})$. The Jacobian $\frac{\partial h(\mathbf{y})}{\partial \mathbf{y}}$ is included in the likelihood and the GP and warping parameters

are learned simultaneously. A common warping functions is the neural net style function:

$$\xi_i = h(y_i) = y_i + \sum_{j=1}^n a_j \tanh(b_j(y_i + c_j)), \quad (3)$$

where $a_j \geq 0, b_j \geq 0, \forall j$ to guarantee monotonicity [34, 38, 54]. Note that we use $\mathbf{h}(\cdot)$ to denote the vector version $\mathbf{h} : \mathbb{R}^n \rightarrow \mathbb{R}^n, \mathbf{h}(\mathbf{y}) = [h(y_1), \dots, h(y_n)]^\top$, which warps each component individually.

2.2 Robust optimization

Robust optimization immunizes optimization problems against parametric uncertainty by requiring constraints with uncertain parameters \tilde{a}_i to hold for all values inside some uncertainty set \mathcal{U} [27]. Application areas range from finance and engineering to scheduling and compressed least squares [6, 27]. The uncertainty set \mathcal{U} can take many different geometries, e.g., box [56], ellipsoidal [9], and polyhedral sets [13]. When \mathcal{U} is convex and the constraint is concave, the semi-infinite constraint can often be reformulated into a deterministic equivalent using duality [8]. The general case can be solved using bilevel optimization [3, 40], but this requires solving the inner maximization problem to global optimality, even to obtain feasible solutions.

2.3 Standard GPs: chance constrained optimization

When $g(\cdot)$ is modeled well by a standard GP, chance constraint Eq. (2) can be exactly replaced by a deterministic equivalent [20]. Since $\{g(\mathbf{y}_i), i \in S\} \sim \mathcal{N}(\boldsymbol{\mu}, \Sigma)$ is normal distributed, the linear combination:

$$\beta = \sum_{i \in S} g(\mathbf{y}_i) x_i$$

is also normal distributed with distribution:

$$\beta \sim \mathcal{N} \left(\sum_{i \in S} \mu_i x_i, \sum_{i, j \in S} x_i \sigma_{i, j}^2 x_j \right).$$

Note that we have suppressed the dependence of $\boldsymbol{\mu}$ and Σ on \mathbf{y}_i for notational simplicity. For a given confidence level α , we can therefore replace chance constraint Eq. (2) by:

$$\sum_{i \in S} \mu_i x_i + F(1 - \alpha) \cdot \sqrt{\sum_{i, j \in S} x_i \sigma_{i, j}^2 x_j} \leq b, \quad (4)$$

where $F(\cdot)$ is the cumulative distribution function of the standard normal distribution. If the GP models $g(\cdot)$ well, Eq. (4) is an exact deterministic reformulation of chance constraint Eq. (2).

2.4 Warped GPs: robust approximation

If $g(\cdot)$ is insufficiently modeled by a standard GP, a warped GP may be a more suitable model [54]. In this case, a direct reformulation of the chance constraint as outlined above for the standard GP case is not known. Such chance constraints are generally addressed by (i) sample approximation [37, 45, 46] or (ii) safe outer-approximation [1, 35, 43, 44, 48, 62]. Instead, we develop a robust approximation. First consider an optimization problem containing a nominal version of Constraint (1):

$$\min_{(\mathbf{x}, \mathbf{y}) \in \mathcal{X}} f(\mathbf{x}, \mathbf{y}) \quad (5a)$$

$$\text{s.t.} \quad \sum_i h^{-1}(\mu(\mathbf{y}_i))x_i \leq b, \quad i \in [n] \quad (5b)$$

where \mathbf{y} is the vector containing all elements of $\mathbf{y}_i, \forall i$. Here, the inversely warped mean prediction of the GP $h^{-1}(\mu(\cdot))$ replaces the black-box function $g(\cdot)$. Clearly, a solution to Problem (5) is not guaranteed to be feasible in practice if the prediction $\mu(\mathbf{y}_i)$ is uncertain. Using the full multivariate distribution generated by the sampling points $\{\mathbf{y}_i\}$, we can construct an α -confidence ellipsoid in the latent space:

$$\mathcal{E}^\alpha(\mathbf{y}) = \{ \xi : (\xi - \boldsymbol{\mu}(\mathbf{y}))^\top \Sigma^{-1}(\mathbf{y}) (\xi - \boldsymbol{\mu}(\mathbf{y})) \leq F_n^{1-\alpha} \}. \quad (6)$$

Here, $F_n^{1-\alpha}$ is the cumulative distribution function of the χ^2 distribution with n degrees of freedom. Assuming that the warped GP models the black-box function well, $\mathcal{E}^\alpha(\mathbf{y})$ contains the true value $h(g(\mathbf{y}_i))$ with probability at least $1 - \alpha$. We therefore construct the following robust optimization problem:

$$\min_{(\mathbf{x}, \mathbf{y}) \in \mathcal{X}} f(\mathbf{x}, \mathbf{y}) \quad (7a)$$

$$\text{s.t.} \quad \mathbf{z}^\top \mathbf{x} \leq b \quad \forall h(\mathbf{z}) \in \mathcal{E}^\alpha(\mathbf{y}) \quad (7b)$$

Any solution to Problem (7) is feasible with probability at least $1 - \alpha$ given that the warped GP models the underlying data generating distribution well. Alternatively, we can take the warping into the uncertainty set:

$$\min_{(\mathbf{x}, \mathbf{y}) \in \mathcal{X}} f(\mathbf{x}, \mathbf{y}) \quad (8a)$$

$$\text{s.t.} \quad \mathbf{z}^\top \mathbf{x} \leq b \quad \forall \mathbf{z} \in \mathcal{U}(\mathbf{y}) \quad (8b)$$

where \mathcal{U} :

$$\mathcal{U}(\mathbf{y}) = \{ \mathbf{z} \in \mathbb{R}^l : (\mathbf{h}(\mathbf{z}) - \boldsymbol{\mu}(\mathbf{y}))^\top \Sigma^{-1}(\mathbf{y}) (\mathbf{h}(\mathbf{z}) - \boldsymbol{\mu}(\mathbf{y})) \leq F_n^{1-\alpha} \}. \quad (9)$$

Note that Problem (8) can also be interpreted as approximating a robust problem

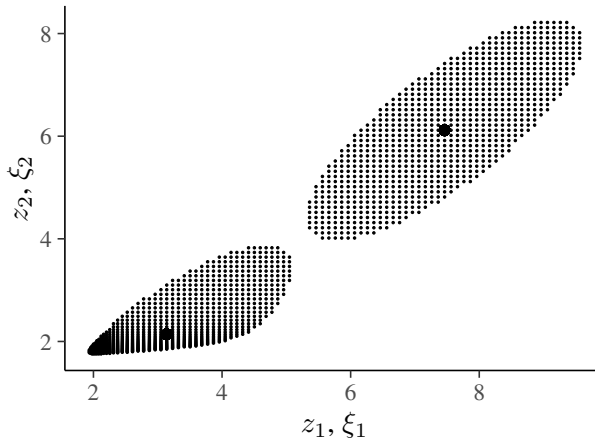


Figure 1: Example of uncertainty sets \mathcal{E}^α in latent and \mathcal{U} in observation space.

with an uncertainty set over functions $\tilde{g} \in \mathcal{U}^g$ (see Theorem (1), Appendix B). Fig. (1) shows an example of the ellipsoidal and warped sets \mathcal{E}^α and \mathcal{U} for $n = 2$. The warped set \mathcal{U} (Eqn. 9) may or may not be convex, depending on the warping function $h(\cdot)$.

2.4.1 Reformulation for convex warped sets \mathcal{U}

In the following we suppress the dependence of $\boldsymbol{\mu}$ and Σ on \mathbf{y} for notational simplicity. We first assume that the warped set \mathcal{U} retains convexity. In this case the inner maximization is convex:

$$\max_{\mathbf{z}} \mathbf{z}^\top \mathbf{x} \quad (10a)$$

$$\text{s.t. } (\mathbf{h}(\mathbf{z}) - \boldsymbol{\mu})^\top \Sigma^{-1} (\mathbf{h}(\mathbf{z}) - \boldsymbol{\mu}) \leq F_n^{1-\alpha}, \quad (10b)$$

Problem (10) generally doesn't have a simple closed form solution. Instead, we can use Wolfe duality to transform Problem (10) into an equivalent minimization

problem, leading to a deterministic reformulation of Problem (8):

$$\min_{(\mathbf{x}, \mathbf{y}) \in X, \mathbf{z}, u} f(\mathbf{x}) \quad (11a)$$

$$\text{s.t. } \mathbf{z}^\top \mathbf{x} + u \cdot ((\mathbf{h}(\mathbf{z}) - \boldsymbol{\mu})^\top \Sigma^{-1} (\mathbf{h}(\mathbf{z}) - \boldsymbol{\mu}) - F_n^{1-\alpha}) \leq b \quad (11b)$$

$$\mathbf{x} + 2u \cdot \nabla \mathbf{h}(\mathbf{z}) \Sigma^{-1} (\mathbf{h}(\mathbf{z}) - \boldsymbol{\mu}) = \mathbf{0} \quad (11c)$$

$$u \geq 0, \quad (11d)$$

where u is a dual variable, $\nabla \mathbf{h}(\mathbf{z}) = \text{diag}(h'(z_i))$, and Constraint (11c) is the Karush-Kuhn-Tucker (KKT) stationarity condition. Note that, unless $\mathbf{x} = \mathbf{0}$, the stationarity condition means that $u \neq 0$ and, due to complementary slackness, $w(\mathbf{z}, \mathbf{y}) = 0$, i.e.:

$$(\mathbf{h}(\mathbf{z}) - \boldsymbol{\mu})^\top \Sigma^{-1} (\mathbf{h}(\mathbf{z}) - \boldsymbol{\mu}) = F_n^{1-\alpha}. \quad (12)$$

Furthermore, we can reformulate Eq. (11c) to:

$$\mathbf{h}(\mathbf{z}) - \boldsymbol{\mu} = -\frac{1}{2u} \Sigma \nabla \mathbf{h}^{-1}(\mathbf{z}) \mathbf{x}$$

Substituting this in Eq. (12) yields:

$$\frac{1}{4u^2} \mathbf{x}^\top \nabla \mathbf{h}^{-1}(\mathbf{z}) \Sigma \nabla \mathbf{h}^{-1}(\mathbf{z}) \mathbf{x} = F_n^{1-\alpha}.$$

This leads to a slightly different formulation which has the advantage that it does not depend on the inverse of the covariance matrix Σ^{-1} :

$$\min_{(\mathbf{x}, \mathbf{y}) \in \mathcal{X}, \mathbf{z}, u} f(\mathbf{x}, \mathbf{y}) \quad (13a)$$

$$\text{s.t. } \mathbf{z}^\top \mathbf{x} \leq b \quad (13b)$$

$$\Sigma \nabla \mathbf{h}^{-1}(\mathbf{z}) \mathbf{x} + 2u \cdot (\mathbf{h}(\mathbf{z}) - \boldsymbol{\mu}) = \mathbf{0} \quad (13c)$$

$$4u^2 F_l^{1-\alpha} = \mathbf{x}^\top \nabla \mathbf{h}^{-1}(\mathbf{z}) \Sigma \nabla \mathbf{h}^{-1}(\mathbf{z}) \mathbf{x} \quad (13d)$$

$$u \geq 0, \quad (13e)$$

where $\nabla \mathbf{h}^{-1}(\mathbf{z})$ is a diagonal matrix containing the inverse elements of $\nabla \mathbf{h}(\mathbf{z})$.

2.4.2 Convexity conditions

Section 2.4.1 relies on the convexity of the inner maximization problem. If \mathcal{U} is non-convex, Problem (13) is not necessarily equivalent to Problem (8) as there may be

more than one KKT point. Since \mathcal{U} is the confidence set of a multivariate distribution, however, may often be convex, especially when the distribution is unimodal. The following section analyzes conditions where the Wolfe duality approach is justified.

First consider the inner maximization Problem (10) transformed into the latent space by substituting $\mathbf{z} = \mathbf{h}^{-1}(\xi)$:

$$\max_{\xi} \quad \mathbf{x}^\top \mathbf{h}^{-1}(\xi) \quad (14a)$$

$$\text{s.t.} \quad (\xi - \boldsymbol{\mu})^\top \Sigma^{-1} (\xi - \boldsymbol{\mu}) \leq F_n^{1-\alpha}, \quad (14b)$$

which depends on the generally not explicitly known inverse warping function h^{-1} . We further state the well known result on the derivative of inverse functions [4]:

Lemma 1. *If $f : \mathbb{R} \rightarrow \mathbb{R}$ is continuous, bijective, and differentiable and $f'(f^{-1}(x)) \neq 0$, then $[f^{-1}]'(x) = \frac{1}{f'(f^{-1}(x))}$.*

Using this, we can show the following proposition.

Theorem 1. *Let the warping function $h(\cdot)$ be concave (convex) and let $x_i \geq 0$ (≤ 0), $\forall i$, then the inner maximization Problem (10) has a unique KKT point.*

Proof. Note that Problem (14) is convex when \mathbf{h}^{-1} is concave (convex) and $x_i \geq 0$ ($x_i \leq 0$), $\forall i$. The KKT conditions for Problems (10) and (14) are:

$$\mathbf{x} + 2u \nabla \mathbf{h}(\mathbf{z}) \Sigma^{-1} (\mathbf{h}(\mathbf{z}) - \boldsymbol{\mu}) = \mathbf{0} \quad (15a)$$

$$(\mathbf{h}(\mathbf{z}) - \boldsymbol{\mu})^\top \Sigma^{-1} (\mathbf{h}(\mathbf{z}) - \boldsymbol{\mu}) = F_n^{1-\alpha} \quad (15b)$$

and:

$$\nabla \mathbf{h}^{-1}(\xi) \mathbf{x} + 2u \Sigma^{-1} (\xi - \boldsymbol{\mu}) = \mathbf{0} \quad (16a)$$

$$(\xi - \boldsymbol{\mu})^\top \Sigma^{-1} (\xi - \boldsymbol{\mu}) = F_n^{1-\alpha}, \quad (16b)$$

where:

$$[\nabla \mathbf{h}^{-1}(\xi)]_{i,j} = \begin{cases} h^{-1}(\xi_i), & i = j \\ 0, & i \neq j \end{cases} \quad (17)$$

By Lemma (1):

$$[\nabla \mathbf{h}^{-1}(\xi)]_{i,j} = \begin{cases} h^{-1}(\xi_i), & i = j \\ 0, & i \neq j \end{cases} = \begin{cases} \frac{1}{h'(h^{-1}(\xi_i))}, & i = j \\ 0, & i \neq j \end{cases} = [\nabla \mathbf{h}(\mathbf{h}^{-1}(\xi))]_{i,j}^{-1}. \quad (18)$$

So Problem 16 is equivalent to:

$$\nabla[\mathbf{h}(\mathbf{h}^{-1}(\xi))]^{-1}\mathbf{x} + 2u\Sigma^{-1}(\xi - \boldsymbol{\mu}) = \mathbf{0} \quad (19a)$$

$$(\xi - \boldsymbol{\mu})^\top \Sigma^{-1}(\mathbf{y} - \boldsymbol{\mu}) = F_n^{1-\alpha}. \quad (19b)$$

Let \mathbf{z}^* be a KKT point for Problem (10), then $\mathbf{y}^* = h(\mathbf{z}^*)$ is clearly a solution to Problem (19), and therefore a KKT point for Problem (14). Since Problem (14) is convex, \mathbf{z}^* is unique. \square

2.4.3 Strategy for non-convex warped sets \mathcal{U}

When \mathcal{U} is non-convex, we need to globally optimize the inner maximization problem efficiently. To this end we develop a custom divide and conquer strategy which makes use of the problems special structure. We first note the following properties of the inner maximization problem.

Lemma 2. *Let \mathbf{z}^* be the solution of Problem 10, then \mathbf{z}^* is on the boundary of \mathcal{U} , i.e., $\mathbf{z}^* \in \partial\mathcal{U}$.*

Proof. See Appendix C. \square

Lemma 3. *The bounding box of an ellipsoid $\mathbf{x}^\top \Sigma^{-1} \mathbf{x} \leq r^2$ is given by the extreme points $x_i = \mu_i \pm r\sigma_{ii}$*

Proof. See Appendix C. \square

Lemma 4. *Consider a version of Problem (14) in which the ellipsoidal feasible region is replaced by its bounding box:*

$$\max_{\xi} \mathbf{x}^\top h^{-1}(\xi) \quad (20a)$$

$$\text{s.t. } \mu_i - r\sigma_{ii} \leq \xi_i \leq \mu_i + r\sigma_{ii} \quad \forall i. \quad (20b)$$

If $x_i \geq 0, \forall i$, the optimal solution ξ^ to this problem is $\xi_i^* = \mu_i + r\sigma_{ii}, \forall i$.*

Proof. Let ξ^* be the optimal solution to Problem (20). Note that ξ^* lies on the boundary of the feasible space (Lemma 6). Assume $\exists i$, s.t., $\xi_i^* < \mu_i + r\sigma_{ii}$. Because h^{-1} is strictly monotonically increasing and $x_i \geq 0$, $x_i h^{-1}(\xi_i) > x_i h^{-1}(\mu_i + r\sigma_{ii})$. Therefore we can construct a new solution $\hat{\xi}$:

$$\hat{\xi}_j = \begin{cases} \xi_j^* & j \neq i \\ \mu_j + r\sigma_{jj} & j = i, \end{cases} \quad (21)$$

for which $\mathbf{x}^\top \hat{\xi} \geq \mathbf{x}^\top \xi^*$, which is a contradiction. \square

Theorem 2. Let $\bar{\xi}(\xi)$ be $\bar{\xi}_i = \mu_i + r\sigma_{ii}$ ($\xi_i = \mu_i - r\sigma_{ii}$) and ξ^* the optimal solution to Problem (14). Then $\mathbf{x}^\top h^{-1}(\xi) \leq \mathbf{x}^\top h^{-1}(\xi^*) \leq \mathbf{x}^\top h^{-1}(\bar{\xi})$.

Proof. The results follows immediately from Lemma (4) because Problem (20) is a relaxation of Problem (14). \square

Using Lemma (6) and Theorem (2) we develop the spatial branching strategy shown in Algorithm (1). It starts by outer-approximating the ellipsoid by its bounding box and evaluating the objective $\mathbf{x}^\top \mathbf{h}^{-1}(\xi)$ at the two corner points $(\underline{\xi}, \bar{\xi})$, obtaining an upper and lower bound (Theorem 2). The algorithm then branches on the dimension of largest width. Boxes can be pruned if they are fully inside or outside the ellipsoid (Lemma 6).

Algorithm 1 Globally optimize inner maximization problem

```

lower bound, upper bound  $\leftarrow \mathbf{x}^\top h^{-1}(\underline{\xi}), \mathbf{x}^\top h^{-1}(\bar{\xi})$ 
nodes  $\leftarrow [(\underline{\xi}, \bar{\xi})]$ 
while (upper bound - lower bound)/upper bound  $\leq \epsilon$  do
   $(\xi, \bar{\xi}) \leftarrow$  choose element in nodes with largest  $\mathbf{x}^\top h^{-1}(\bar{\xi})$ 
  upper bound  $\leftarrow \mathbf{x}^\top h^{-1}(\bar{\xi})$ 
  children  $\leftarrow$  split  $(\xi, \bar{\xi})$  along single axis
  for  $(\xi, \bar{\xi})$  in children do
    if  $(\xi, \bar{\xi})$  contains boundary point of ellipsoid and lower bound  $\leq \mathbf{x}^\top h^{-1}(\bar{\xi})$ 
    then
      add  $(\xi, \bar{\xi})$  to nodes
      lower bound  $\leftarrow \min\{\mathbf{x}^\top h^{-1}(\xi), \text{lower bound}\}$ 
    end if
  end for
end while

```

2.5 Iterative a posteriori approximation

The a priori probabilistic bound implied by \mathcal{E}^α may be overly conservative. Alg. (2) is an alternative, less conservative strategy that iteratively determines the uncertainty set size. Starting with the confidence level α equal to the target feasibility ϵ_0 , Alg. (2) iteratively solves the robust optimization problem, evaluates the feasibility of the obtained solution using the distribution of the warped GP to generate random realizations, and consequently adjusts the confidence level α using bisection

Algorithm 2 Posteriori approximation

```
1:  $\alpha \leftarrow \epsilon_0$ 
2: while  $\|\epsilon - \epsilon_0\| \geq \delta$  do
3:    $\mathbf{x} \leftarrow$  solution of Problem (13) with  $\alpha$ 
4:    $\epsilon \leftarrow$  estimated feasibility of  $\mathbf{x}$ 
5:   if  $\epsilon - \epsilon_0 \geq 0$  then
6:      $\alpha_U \leftarrow \alpha, \epsilon_U \leftarrow \epsilon$ 
7:   else
8:      $\alpha_L \leftarrow \alpha, \epsilon_L \leftarrow \epsilon$ 
9:   end if
10:   $\alpha \leftarrow \frac{\alpha_L + \alpha_U}{2}$  {Bisection search}
11: end while
```

search. The search terminates when a solution has been found that is sufficiently close (tolerance δ) to the target feasibility ϵ_0 .

3 Case studies

3.1 Production planning

Our first case study is inspired by production planning. Assume that a company wants to decide how much product x_t to produce in a number of subsequent time periods $\mathbf{x} = [x_1, \dots, x_t, \dots, x_T]$. There is a known cost of production c_t which may vary from period to period. The company seeks to maximize its profit ψ , which depends on the total production cost $\sum_t c_t x_t$ and revenue $\sum_t \tilde{p}_t x_t$. Here \tilde{p}_t is the price at which the product can be sold in period t . The company has to sell all its product in the same time period, e.g., because the product is perishable. The sale price depends on the amount the company produces in that period $\tilde{p}_t = \tilde{p}(x_t)$, e.g., because the company has a very large market share.

The company uses GP regression to predict $\tilde{p}(x_t)$ based on limited historical data. Additional features, e.g., season and general state of the economy, could be part of this regression but are irrelevant for our purpose as they are not decision variables. The prediction has to be considered uncertain and the company wants a production plan guaranteeing a certain profit with some confidence. This decision problem can

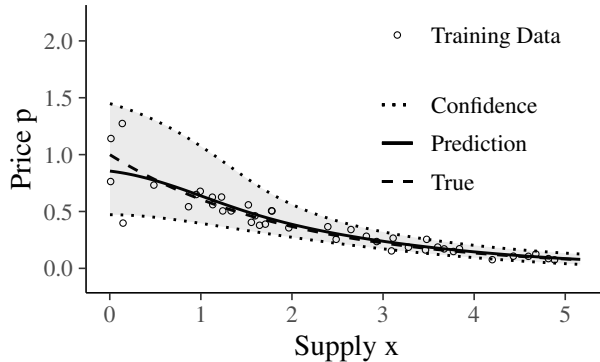


Figure 2: GP trained using 50 observations from the price-supply curve $p(x_t) = \exp(-x_t) + \epsilon$ with non-uniform Gaussian noise $\epsilon \sim \mathcal{N}(0, 4 \cdot 0.3 \cdot \exp(-x/2))$. The confidence region is two standard deviations wide.

be formulated as a chance constrained optimization problem:

$$\max_{\mathbf{x} \in \mathbb{R}^T, \psi} \psi \quad (22a)$$

$$\text{s.t. } P \left(\sum_{t=1}^T (\tilde{p}(x_t) - c_t) x_t \geq \psi \right) \geq 1 - \alpha \quad (22b)$$

Choosing $p(x_t) = \exp(-x_t)$ as ground truth for the price-supply curve, we generate noisy data $\tilde{p}(x_t) = p(x_t) + \epsilon$ and fit a GP surrogate as shown in Fig. (2). We consider uniform Gaussian noise ($\epsilon \sim \mathcal{N}(0, \sigma_{\text{noise}})$) and non-uniform Gaussian noise ($\epsilon \sim \mathcal{N}(0, 4 \cdot \sigma_{\text{noise}} \cdot \exp(-x/2))$), where σ_{noise} is a parameter determining the amount of noise. We use a squared exponential kernel for this case study, but the proposed method does not generally rely on a specific choice for $k(\cdot, \cdot)$.

3.2 Drill scheduling

The objective in drilling oil wells is generally minimizing total well completion time. The aim of the drill scheduling problem, illustrated in Fig. (??), is to find a schedule of the two decision variables, rotational speed $\dot{N} \in \mathbb{R}$ and weight on bit $W \in \mathbb{R}$, as a function of depth $x \in \mathbb{R}$. Current practice often consists of minimizing the total drilling time, which depends on \dot{N} and W through a non-linear bit-rock interaction model [22] and the motor's power-curves (see Appendix D). Total well completion time, however, also depends on maintenance time. Current practice may increase

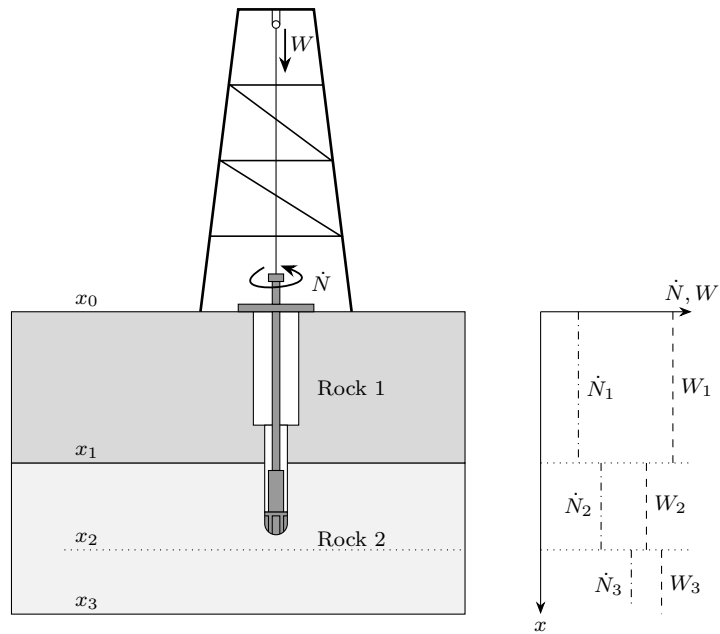


Figure 3: Illustration of drill scheduling problem with two rock types. The rock type changes at x_1 , maintenance is scheduled at x_2 , and the target depth is x_3 . The right side shows an example schedule of the decision variables \dot{N} and W .

maintenance time because drilling quickly can detrimentally effect motor degradation. Furthermore, the motors degradation characteristics are subject to uncertainty and are often obtained through a mixture of experiments and expensive numerical simulations [2]. Other works have considered uncertain equipment degradation in scheduling applications [60, 5], but not with predicted degradation rates.

To find the optimal trade off between drilling and maintenance time, we propose a drill scheduling model which explicitly considers uncertainty in the motor degradation characteristics. First consider a model which discretizes the drill trajectory into n equidistant intervals:

$$\min_{\mathbf{W}, \dot{N}, \mathbf{z}, \mathbf{y}, \mathbf{V}, \Delta \mathbf{p}, \mathbf{R}} \sum_{i=1}^n \left(\frac{\Delta x_i}{V_i} + z_i \Delta t_i^{\text{maint}} \right) \quad (23a)$$

$$\text{s.t } V_i = f(\dot{N}_i^{\text{top}}, W_i, \Delta p_i) \quad \forall i \in [n] \quad (23b)$$

$$0 \leq R_i = \sum_{j=1}^i \left(\frac{\Delta x_j}{V_j} \cdot r(\Delta p_j) - y_j \right) \leq 1 \quad \forall i \in [n] \quad (23c)$$

$$z_i \geq y_i, z_i \in \{0, 1\} \quad \forall i \in [n], \quad (23d)$$

The rate of penetration V_i in each segment depends on the drill parameters (\dot{N}_i and W_i) through the non-linear model in Appendix D. The rate of degradation $r(\cdot)$ is a black-box function of the differential pressure across the motor Δp . We model $r(\cdot)$ with a warped GP based on 10 data points from a curve obtained by Ba et al. [2] through a combination of experiments and numerical simulation. The maintenance indicator R_i keeps track of the total cumulative degradation of the motor. We assume the motor fails when R_i reaches 1. Binary variable z_i indicates whether maintenance is scheduled in segment i . If maintenance is scheduled, the continuous variable y_i resets the total degradation indicator R_i to zero. Note that the bit-rock interaction model depends on rock parameters which can change from segment to segment.

A major disadvantage of Model (23) is that it requires a large number of segments in order to get a good resolution on the optimal maintenance depth. To avoid this we propose, in analogy with continuous time formulations [52, 24], an alternative

continuous depth scheduling formulation:

$$\min_{\mathbf{W}, \mathbf{N}, \mathbf{x}, \Delta \mathbf{p}, \mathbf{V}, \mathbf{R}} \sum_{i \in N} \left(\frac{x_i - x_{i-1}}{V_i} \right) + \sum_{m \in M} \Delta t^{\text{maint}}(x_m) \quad (24a)$$

$$\text{s.t } V_i = f(\dot{N}_i, W_i, \Delta p_i) \quad \forall i \in N = [n] \quad (24b)$$

$$R_m = \sum_{j=m^-}^m \left(\frac{x_j - x_{j-1}}{V_j} \cdot r(\Delta p_j) \right) \leq 1 \quad \forall m \in M \cup \{n\} \quad (24c)$$

Model (24) only considers geological segments (segments with constant rock parameters) and maintenance induced segments. The vector \mathbf{x} is ordered and contains the fixed rock formation depths as well as the variable maintenance depths. Fig. (??) shows an example where x_1 is the fixed depth at which the geology changes and x_2 is the variable depth of a maintenance event. The indices $i \in M$ of the variable maintenance depths are determined a priori, i.e., we decide both the number of maintenance events as well as the geological segment in which they occur a priori. m^- is either the index of the previous maintenance event or 1 if m is the first element in M .

While Problem (24) cannot decide the optimal number of maintenance events, it is easier to solve than Problem (23) because it does not contain integer variables and generally has a much smaller number of segments, i.e., fewer variables and constraints. The following discusses strategies for deciding the optimal number and segment assignment of maintenance events.

3.2.1 Integer strategy

In drill scheduling, the number of maintenance events n is generally small ($n \leq 4$). The number of geological segments m can be large in practice but will not be known a priori. We therefore consider groupings of segments into a small number ($m \leq 10$) of longer segments with average rock parameters which are known a priori. Given n and m , the combinatorial complexity of enumerating the maintenance-segment assignment problem is $N == \binom{n+m-1}{m}$. However, the optimal number of maintenance events m is a decision variable. Therefore, finding the globally optimal maintenance-segment assignment also requires enumerating different values of m .

Alg. (3) derives upper bounds for the number of maintenance events m as well as their location. It starts by solving Problem (24) without any maintenance events and ignoring the upper bound on the degradation indicator $R_n \not\leq 1$. The floor of the maintenance indicator at the target depth x_n , $\lfloor R_n \rfloor$ is an upper bound for the necessary number of maintenance events m . Alg. (3) then starts at the target depth x_n and inserts $\lfloor R_n \rfloor$ maintenance events at the earliest possible points that satisfy

Algorithm 3 Deriving upper bounds for m and x_m

- 1: $\mathbf{x}, \mathbf{R}, \hat{\mathbf{V}} \leftarrow$ solve Problem (24) without Constraint (24c), $M = \emptyset$
 - 2: $\hat{M} \leftarrow \{1, \dots, \lfloor R_n \rfloor\}$
 - 3: **for** $m \in \{\lfloor R_n \rfloor, \dots, 0\}$ **do**
 - 4: $\hat{x}_m \leftarrow \arg \min_{x_m} \sum_{j=m}^{m^+} \left(\frac{x_j - x_{j-1}}{V_j} \cdot r(\Delta p_j) \right)$
 - 5: **end for**
-

the maintenance constraint. The locations \hat{x}_m are upper bounds for the maintenance locations:

Lemma 5. *Let (M^*, \mathbf{x}^*) be the globally optimal maintenance-segment assignment. Let $(\hat{M}, \hat{\mathbf{x}})$ be determined by Alg. (3). If i^* and \hat{i} are the i -th last elements in M^* and \hat{M} respectively, then $x_{i^*}^* \leq \hat{x}_{\hat{i}}$.*

Proof. Let j^* and \hat{j} be the $(i+1)$ -th last elements in M^* and \hat{M} respectively. Assume $x_{i^*}^* \leq \hat{x}_{\hat{i}}$ but $x_{j^*}^* > \hat{x}_{\hat{j}}$. Construct a new solution $(M', \mathbf{x}', \mathbf{V}')$ by moving $x_{j^*}^*$ to $\hat{x}_{\hat{j}}$ and drilling at maximum speed $\hat{V}_{\hat{j}}$ between $\hat{x}_{\hat{j}}$ and $x_{i^*}^*$:

$$M' = M^*, x'_k = \begin{cases} x_k^* & k \neq j^*, k \in M' \\ \hat{x}_k & k = j^*, k \in M' \end{cases}, \mathbf{V}' = \begin{cases} V_k^* & k \neq j^*, k \in M' \\ \hat{V}_k & k = j^*, k \in M' \end{cases}.$$

$(M', \mathbf{x}', \mathbf{V}')$ has drilling and maintenance cost lower than $(M^*, \mathbf{x}^*, \mathbf{V}^*)$, which is a contradiction. Therefore $x_{i^*}^* \leq \hat{x}_{\hat{i}} \implies x_{j^*}^* \leq \hat{x}_{\hat{j}}$. Furthermore, note that $x_{i^*}^* \leq \hat{x}_{\hat{i}}$ has to be true for the last maintenance event by the same logic as above. The proposition follows by induction. \square \square

Lemma (5) reduces the number of maintenance-segment assignments to enumerate:

Note 1. *Let $\hat{\mathbf{x}}$ be the upper bounds on maintenance locations from Alg. (3). Let n_i be the segment containing \hat{x}_i . The complexity of enumerating the maintenance-segment assignment problem using the upper bounds from Alg. (3) is:*

$$N = \sum_{i_1=1}^{n_1} \sum_{i_2=i_1}^{n_2} \dots \sum_{i_m=i_{m-1}}^{n_m} 1 = \sum_{i_1=1}^{n_1} \sum_{i_2=i_1}^{n_2} \dots \sum_{i_{m-1}=i_{m-2}}^{n_{m-1}} n_m - i_{m-1} + 1.$$

3.2.2 Heuristics

Alg. (3) is equivalent to minimizing the drilling cost without considering degradation — a strategy often used in practice. It provides feasible but likely suboptimal solutions to Problem (24), i.e., it can be used as a heuristic. We call this the *no-degradation heuristic* and propose a second, improved heuristic: the *boundary heuristic*, outlined in Alg. (4). Alg. (4) starts with the solution of the no-degradation heuristic (Alg. 3). It improves the solution by iteratively solving Problem (24) and reassigning maintenance events occurring at geological boundaries to the adjacent segment. It terminates after finding a solution with all maintenance events occurring in the interior of their segment. Note that moving a maintenance event occurring at

Algorithm 4 Boundary heuristic

- 1: $\hat{M} \leftarrow$ no-degradation heuristic (Alg. 3)
 - 2: $\mathbf{x} \leftarrow$ solve Problem (24) with $M = \hat{M}$
 - 3: **while** $\exists m \in M$, s.t. x_m at geological boundary **do**
 - 4: $\hat{M} \leftarrow$ reassign m to neighboring segment, drop maintenance event if at x_0 .
 - 5: $\mathbf{x} \leftarrow$ solve Problem (24) with $M = \hat{M}$
 - 6: **end while**
-

a geological boundary to the adjacent segment cannot lead to a worse solution, i.e. Alg. (4) is an anytime algorithm.

While it does not guarantee global optimality of the maintenance-segment assignment, the boundary heuristic may be useful for very large instances when enumeration is prohibitive.

4 Results

The deterministic reformulations of both case studies were implemented in Pyomo (Version 5.6.8) [32, 31], an algebraic modeling language for expressing optimization problems. As part of this work, we developed a Python (Version 3.6.8) module which takes a GP model trained using the Python library GPy (Version 1.9.6) [28] and predicts $\mu(\mathbf{x})$ and $\Sigma(\mathbf{x})$ as Pyomo expressions (will be available open source on GitHub). This allows the easy incorporation of GP models into Pyomo optimization models. We use the interior-point convex optimization solver Ipopt [59] with a multistart strategy to solve the problem. Each instance was solved 30 times with a random starting point. The multistart procedure ends prematurely if it finds the same optimal solution (with a relative tolerance of 10^{-4}) 5 times.

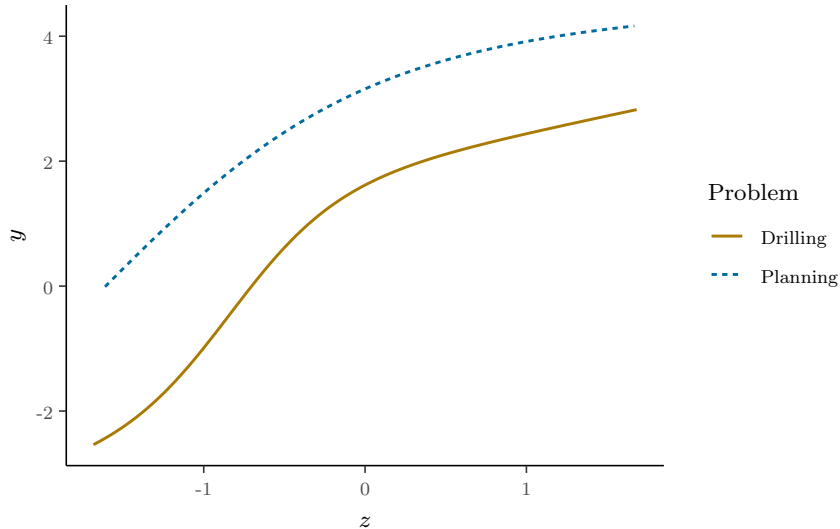


Figure 4: Warping functions for the drilling and production planning case studies. Input values are normalized to zero mean and $\sigma = 1$.

Fig. (4) shows the warping functions for both case studies. Since the production planning warping function is concave and the production amounts x_t are strictly positive, Theorem (1) applies and the warped set \mathcal{U} is convex. Theorem (1) cannot be applied to the drill scheduling case, because its warping function is neither convex nor concave. However, because the warping function is only slightly non-convex, the warped set \mathcal{U} may still be convex for many instances. To avoid solving the bilevel problem directly we therefore use the following strategy: (i) solve the robust reformulation (Eq. 13), (ii) check feasibility of the obtained solution using Algorithm (1) (to a tolerance of 10^{-2}), and (iii) only solve the bilevel problem (Eq. 8) directly if the obtained solution is infeasible. For the instances considered in this work, the obtained solution always turns out to be feasible.

4.1 Production planning

For the production planning case study, we consider 4 model instances with $T = 1, 2, 3$ and 6 time periods. Table (1) shows the cost of production \mathbf{c} . We solve each instance for 30 different confidence values $1 - \alpha$. The GP was trained based on 50 randomly generated data points using both uniform and non-uniform Gaussian noise with $\sigma_{\text{noise}} = 0.01, 0.03, 0.05$, and 0.08.

Period	1	2	3	4	5	6
Cost	0.1	0.05	0.01	0.02	0.1	0.15
Period	7	8	9	10	11	12
Cost	0.04	0.03	0.1	0.11	0.25	0.1

Table 1: Production costs c_t for each time period t .

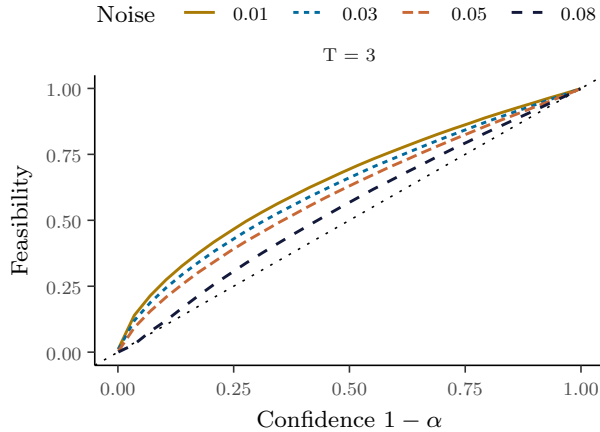


Figure 5: Fraction of feasible solutions as a function of confidence $1 - \alpha$ for the planning problem with three time periods. $1 - \alpha = 0$ corresponds to the nominal case and $1 - \alpha = 1$ to 0% chance of constraint violation. The noise in the data is uniform Gaussian with $\sigma_{\text{noise}} = 0.01, 0.03, 0.05$ and 0.08 and a standard GP model was used. The smaller the noise, the closer the actual feasibility is to the expected confidence (dotted line).

Standard GP: Fig. (5) shows results for the chance constrained approach using a standard GP model. We plot the fraction of feasible scenarios out of 1 million random samples from the true underlying distribution. Fig. (5) shows results for four different noise scenarios. By varying the confidence $1 - \alpha$, we adjust the robustness of the obtained solution. Clearly, the resulting feasibility does not exactly match the expected feasibility (shown as a dotted line) determined by the confidence level $1 - \alpha$. This is due to a mismatch between the true underlying distribution and the normal distribution estimated by the GP. As the amount of noise increases, the GP estimate deteriorates and the mismatch between feasibility and confidence increases.

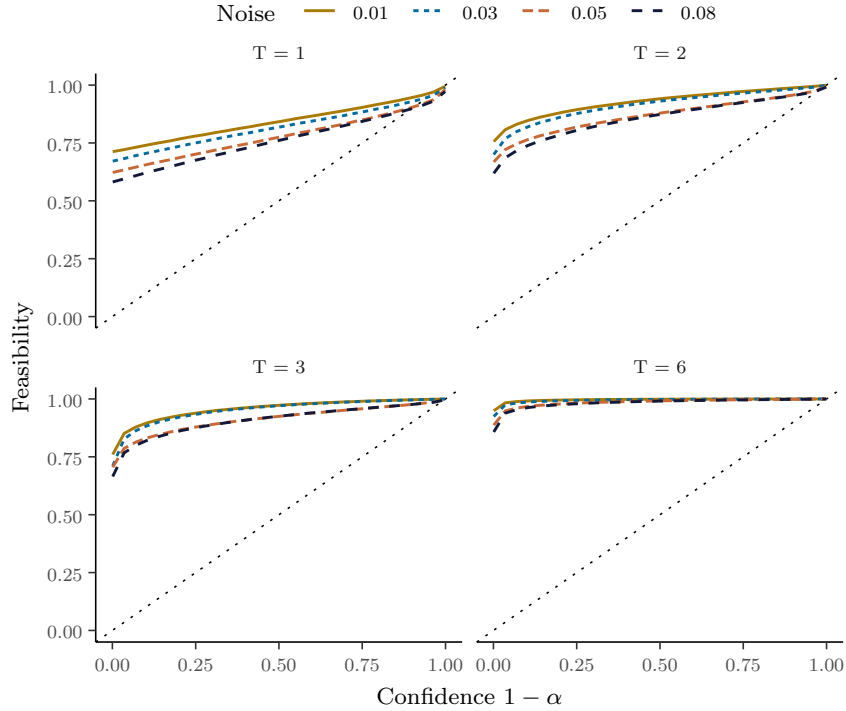


Figure 6: Fraction of feasible solutions as a function of confidence $1 - \alpha$ for non-uniform Gaussian noise with $\sigma_{\text{noise}} = 0.01, 0.03, 0.05$, and 0.08 . Results are shown for four different numbers of time periods $T = 1, 2, 3$ and 6 . The dotted line shows the a priori bound. With increasing numbers of time periods, the robust approximation becomes increasingly conservative.

Warped GP: Fig. (6) shows solution feasibility as a function of confidence $1 - \alpha$ for non-uniform noise using a warped GP model and the proposed robust approach. We show results for four different numbers of time periods. In the nominal case ($1 - \alpha = 0$), the feasibility is always close to 50% because a solution which is valid for the mean price-supply curve will also be valid for many scenarios with higher prices. In the robust case, as expected, feasibility increases as the size of the uncertainty set, i.e. $1 - \alpha$, increases. Notice that the robust approach is almost always a conservative approximation to the chance constraint, as the achieved feasibility is generally larger than the confidence $1 - \alpha$. Small violations of the a priori bound (dotted line) can still occur due to a mismatch between the GP model and the true underlying data generating distribution. The solution conservatism also varies with the number of time periods considered. The a priori bound relaxes as T increases.

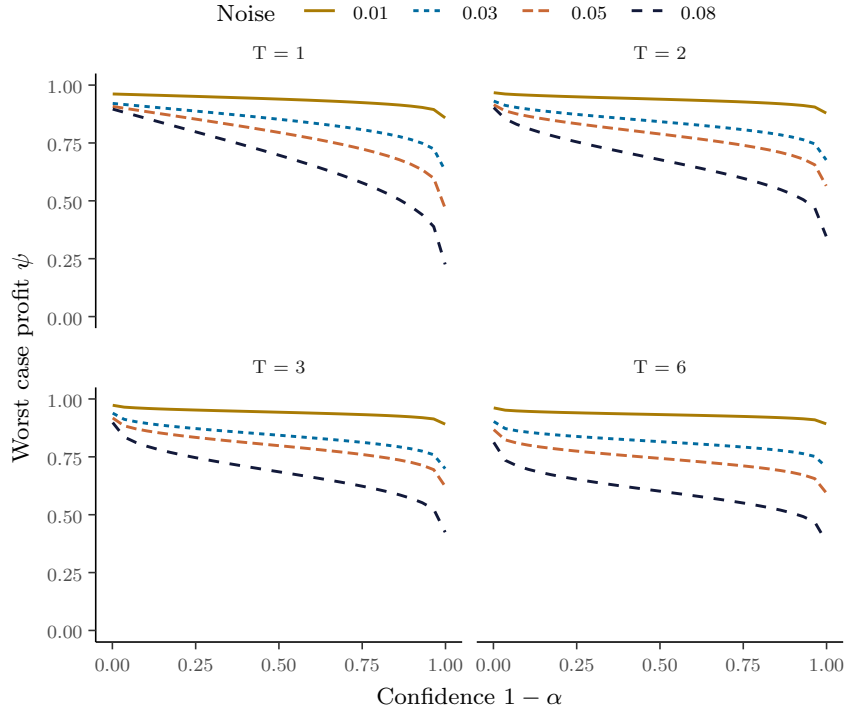


Figure 7: Profit, normalized with respect to nominal profit with $\sigma_{\text{noise}} = 0.01$ (objective of Problem (5)), as a function of confidence $1 - \alpha$ for four different noise scenarios and time periods $T = 1, 2, 3$ and 6. As expected, the objective value decreases with increasing confidence $1 - \alpha$, because more extreme worst case scenarios are considered.

Fig. (7) shows the worst case profit, normalized with respect to the nominal profit for $\sigma_{\text{noise}} = 0.01$, achieved as a function of the confidence level $1 - \alpha$. As expected, increasing the confidence $1 - \alpha$ leads to a lower worst case profit, because a larger confidence hedges against more uncertain price outcomes. Note that results are shown for values of $1 - \alpha$ between 0.001 and 0.999. At $1 - \alpha = 1$, the profit is always zero, because the uncertainty set includes negative prices and the optimal solution is to not produce anything. For a fixed confidence level, noisier data will generally lead to a smaller objective value as there is more uncertainty to hedge against.

Iterative procedure: Finally, Fig. (8) shows solution feasibility for the iterative a posteriori procedure (Alg. 2). We use confidence values between 0.55 and 0.999, since smaller confidences can often not be achieved using the iterative approach

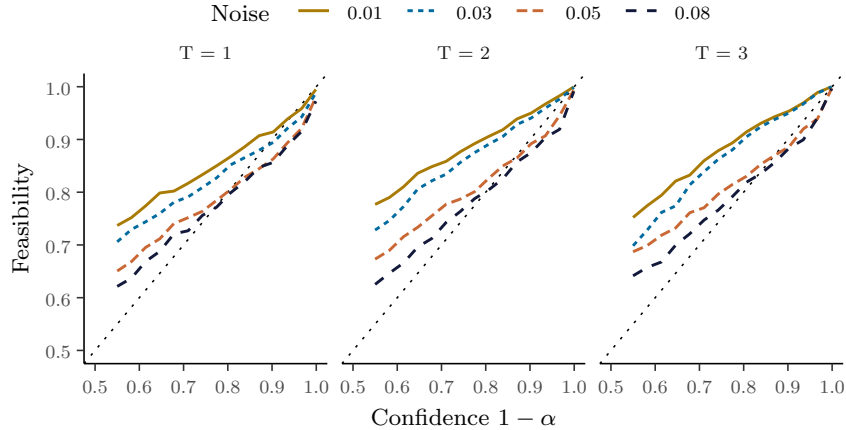


Figure 8: Fraction of feasible solutions vs confidence $1 - \alpha$ for the iterative a posteriori procedure (Alg. 2). If the noise is small, feasibility generally tracks the expected confidence (dotted line) well. For larger noise, deviations can occur due to mismatch between the warped GP model and the true data generating distribution.

(the smallest achievable confidence is the feasibility of the nominal solution, i.e., $\sim 50\%$). The a posteriori approach is clearly less conservative than the a priori approach, however, this comes at the cost of additional computational expense and also potential bound violations when the warped GP does not model the underlying distribution perfectly. The a posteriori approach could therefore be a viable less conservative alternative in relatively low noise scenarios or when more training data is available.

4.2 Drill scheduling

For the drill scheduling case study, we consider two different geologies with 2 and 6 geological segments. We consider a range of target depths and confidence values. Fig. (9) shows the drilling, maintenance, and total cost for a target depth of 2200m as a function of the confidence parameter $1 - \alpha$. In the deterministic case ($1 - \alpha = 0.5$), the optimal strategy is to not do maintenance at all and drill as fast as possible. As we increase $1 - \alpha$ to obtain more robust solutions, we eventually reach a point where the average rate of penetration is slightly lower in order to reduce degradation and guarantee that the well can be completed without a motor failure. For the 2-segment geology the increased cost of drilling outweighs the zero maintenance cost at around $1 - \alpha = 0.92$. After this point the optimal strategy is to do maintenance once.

Results are shown for both the no-degradation and boundary heuristics as well as total enumeration. For this instance, the boundary heuristic leads to the same solution as the globally optimal enumeration strategy. The no-degradation heuristic, on the other hand, leads to suboptimal solutions when the optimal maintenance number is lower than the upper bound $\lfloor R_n \rfloor$.

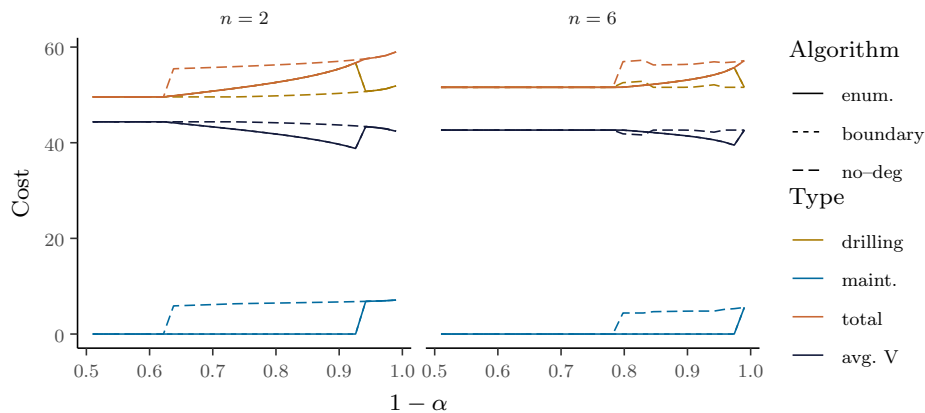


Figure 9: Cost of drilling to a depth of 2200 meters through a geologies with 2 and 6 segments for different values of confidence parameter α . Results are shown for three different integer strategies. The boundary heuristic gives the same results as total enumeration, while the no-degradation heuristic gives suboptimal solutions.

Fig. (10) shows the same cost components as Fig. (9) as a function of the target depth x_n . Results are shown for three different values of $1 - \alpha$ (0.5, 0.75, and 0.99). A larger confidence always leads to a higher cost, as would be expected, but the difference between the deterministic solution and a 99%-confidence robust solution can be larger or small, depending on the target depth, e.g., for a target depth of $x_n = 3000\text{m}$ hedging against uncertainty does not lead to significant cost increases.

Finally, Fig. (11) shows the total solution time for the three integer strategies for the instance with 6 geological segments as a function of confidence parameter $1 - \alpha$. While the no-degradation heuristic often leads to suboptimal solutions, as seen above, it is computationally very cheap. The boundary heuristic comprises a good compromise: it frequently finds the global optimum while being much cheaper computationally. Especially for instances with many geological segments and maintenance events, where the combinatorial complexity of the enumeration strategy becomes prohibitive, it may therefore be a good alternative.

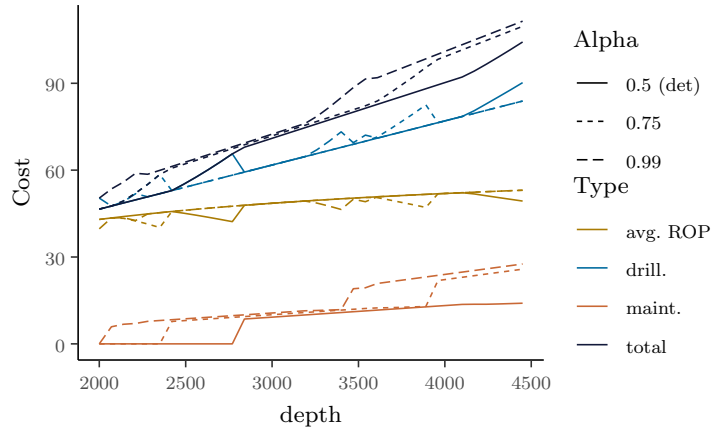


Figure 10: Cost of drilling as a function of target depth for three different for a geology with two rock types for and for three different values of confidence parameter α . All results are obtained with the globally optimal enumeration strategy.

5 Conclusion

Our approach reformulates uncertain black-box constraints, modeled by warped Gaussian processes, into deterministic constraints guaranteed to hold with a given confidence. We achieve this deterministic reformulation of chance constraints by constructing confidence ellipsoids and utilizing Wolfe duality. We show that this approach allows the solution conservatism to be controlled by a sensible confidence probability choice. This could be especially useful in safety-critical settings where constraint violations should be avoided.

References

- [1] Ahmed, S.: Convex relaxations of chance constrained optimization problems. *Optimization Letters* **8**(1), 1–12 (2014)
- [2] BA, S., Pushkarev, M., Kolyshkin, A., Song, L., Yin, L.L.: Positive Displacement Motor Modeling: Skyrocketing the Way We Design, Select, and Operate Mud Motors. In: Abu Dhabi International Petroleum Exhibition & Conference, Dd. Society of Petroleum Engineers (2016)
- [3] Bard, J.F.: Practical Bilevel Optimization, *Nonconvex Optimization and Its Applications*, vol. 30. Springer US, Boston, MA (1998)

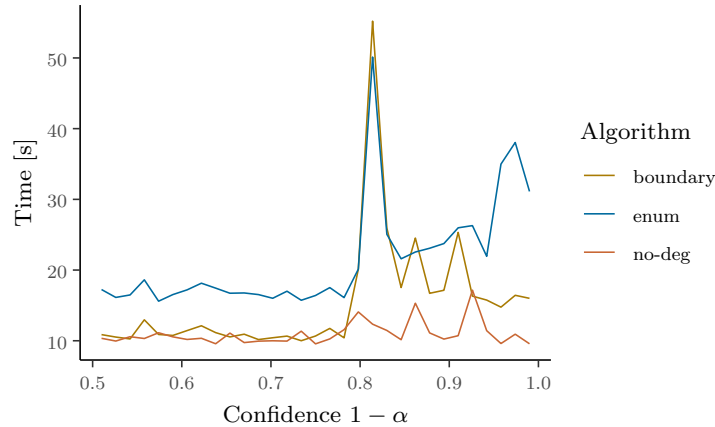


Figure 11: Total time to solve instance with 6 rock types as a function of confidence parameter alpha. While the enumeration strategy is the only approach which is guaranteed to find the globally optimal solution, the boundary heuristic often finds the same solution in significantly less time.

- [4] Baxandall, P.R., Liebeck, H.: Vector calculus, dover ed. edn. Dover Publications, Mineola, N.Y. (2008)
- [5] Baçiftci, B., Ahmed, S., Gebraeel, N., Yildirim, M.: Integrated Generator Maintenance and Operations Scheduling under Uncertain Failure Times. IEEE Transactions on Power Systems (2018)
- [6] Becker, S., Kawas, B., Petrik, M.: Robust partially-compressed least-squares. In: AAAI (2017)
- [7] Beland, J.J., Nair, P.B.: Bayesian Optimization Under Uncertainty. In: NIPS (2017)
- [8] Ben-Tal, A., den Hertog, D., Vial, J.P.: Deriving robust counterparts of nonlinear uncertain inequalities. Math. Program. **149**(1-2), 265–299 (2014)
- [9] Ben-Tal, A., Nemirovski, A.: Robust solutions of Linear Programming problems contaminated with uncertain data. Math. Program. **88**(3), 411–424 (2000)
- [10] Bertsimas, D., Brown, D.B., Caramanis, C.: Theory and Applications of Robust Optimization. SIAM Review **53**(3), 464–501 (2011)

- [11] Bertsimas, D., Nohadani, O., Teo, K.M.: Nonconvex robust optimization for problems with constraints. *INFORMS J. Comput.* **22**(1), 44–58 (2010)
- [12] Bertsimas, D., Nohadani, O., Teo, K.M.: Robust Optimization for Unconstrained Simulation-Based Problems. *Oper. Res.* **58**(1), 161–178 (2010)
- [13] Bertsimas, D., Sim, M.: The Price of Robustness. *Oper. Res.* **52**(1), 35–53 (2004)
- [14] Beykal, B., Boukouvala, F., Floudas, C.A., Sorek, N., Zalavadia, H., Gildin, E.: Global optimization of grey-box computational systems using surrogate functions and application to highly constrained oil-field operations. *Computers and Chemical Engineering* **114**, 99–110 (2018)
- [15] Bhosekar, A., Ierapetritou, M.: Advances in surrogate based modeling, feasibility analysis, and optimization: A review. *Comput. Chem. Eng.* **108**, 250–267 (2018)
- [16] Birge, J.R., Louveaux, F.: *Introduction to Stochastic Programming* (2011)
- [17] Bogunovic, I., Scarlett, J., Jegelka, S., Cevher, V.: Adversarially Robust Optimization with Gaussian Processes. In: *NIPS* (2018)
- [18] Boukouvala, F., Floudas, C.A.: ARGONAUT: AlgoRithms for Global Optimization of coNstrAined grey-box compUTational problems. *Optimization Letters* **11**(5), 895–913 (2017)
- [19] Boukouvala, F., Misener, R., Floudas, C.A.: Global optimization advances in Mixed-Integer Nonlinear Programming, MINLP, and Constrained Derivative-Free Optimization, CDFO. *European Journal of Operational Research* **252**(3), 701–727 (2016)
- [20] Charnes, A., Cooper, W.W.: Deterministic Equivalents for Optimizing and Satisficing under Chance Constraints. *Operations Research* **11**(1), 18–39 (1963)
- [21] Deisenroth, M.P., Fox, D., Rasmussen, C.E.: Gaussian Processes for Data-Efficient Learning in Robotics and Control. *IEEE Transactions on Pattern Analysis and Machine Intelligence* **37**(2), 408–423 (2015)
- [22] Detournay, E., Richard, T., Shepherd, M.: Drilling response of drag bits: Theory and experiment. *International Journal of Rock Mechanics and Mining Sciences* **45**(8), 1347–1360 (2008)

- [23] Dolatnia, N., Fern, A., Fern, X.: Bayesian Optimization with Resource Constraints and Production. Twenty-Sixth International Conference on Automated Planning and Scheduling (ICAPS) (Icaps), 115–123 (2016)
- [24] Floudas, C.A., Lin, X.: Continuous-time versus discrete-time approaches for scheduling of chemical processes: A review. *Computers and Chemical Engineering* **28**(11), 2109–2129 (2004)
- [25] Gardner, J.R., Kusner, M.J., Xu, Z., Weinberger, K.Q., Cunningham, J.P.: Bayesian optimization with inequality constraints. In: ICML (2014)
- [26] Gelbart, M.A., Snoek, J., Adams, R.P.: Bayesian Optimization with Unknown Constraints. arXiv e-prints arXiv:1403.5607 (2014)
- [27] Gorissen, B.L., Yanikolu, I., den Hertog, D.: A practical guide to robust optimization. *Omega (United Kingdom)* **53**, 124–137 (2015)
- [28] GPy: GPy: A Gaussian process framework in python. <http://github.com/SheffieldML/GPy> (since 2012)
- [29] Griffiths, R.R., Hernández-Lobato, J.M.: Constrained Bayesian Optimization for Automatic Chemical Design. In: 32nd Conference on Neural Information Processing Systems (NIPS 2018) (2018)
- [30] Grossmann, I.E.: Pyrolysis of Heavy Oil in the Presence of Supercritical Water: The Reaction Kinetics in Different Phases. *AIChE Journal* **61**(3), 857–866 (2015)
- [31] Hart, W.E., Laird, C.D., Watson, J.P., Woodruff, D.L., Hackebeil, G.A., Nicholson, B.L., Siirola, J.D.: *Pyomo—optimization modeling in python*, vol. 67, second edn. Springer Science & Business Media (2017)
- [32] Hart, W.E., Watson, J.P., Woodruff, D.L.: Pyomo: Modeling and solving mathematical programs in Python. *Mathematical Programming Computation* **3**(3), 219–260 (2011)
- [33] Hüllen, G., Zhai, J., Kim, S.H., Sinha, A., Realff, M.J., Boukouvala, F.: Managing Uncertainty in Data-Driven Simulation-Based Optimization. *Computers & Chemical Engineering* p. 106519 (2019)
- [34] Kou, P., Gao, F., Guan, X.: Sparse online warped Gaussian process for wind power probabilistic forecasting. *Applied Energy* **108**, 410–428 (2013)

- [35] Li, Z., Li, Z.: Optimal robust optimization approximation for chance constrained optimization problem. *Computers and Chemical Engineering* **74**, 89–99 (2015). DOI 10.1016/j.compchemeng.2015.01.003. URL <http://dx.doi.org/10.1016/j.compchemeng.2015.01.003>
- [36] Liu, S., Yue, Y., Krishnan, R.: Adaptive collective routing using Gaussian process dynamic congestion models. In: *Proceedings of the 19th ACM SIGKDD international conference on Knowledge discovery and data mining - KDD '13*, p. 704. ACM Press (2013)
- [37] Luedtke, J., Ahmed, S.: A sample approximation approach for optimization with probabilistic constraints. *SIAM Journal on Optimization* **19**(2), 674–699 (2008)
- [38] Mateo-Sanchis, A., Muñoz-Marí, J., Pérez-Suay, A., Camps-Valls, G.: Warped Gaussian Processes in Remote Sensing Parameter Estimation and Causal Inference. *IEEE Geoscience and Remote Sensing Letters* **15**(11), 1647–1651 (2018)
- [39] Mistry, M., Letsios, D., Krennrich, G., Lee, R.M., Misener, R.: *Mixed-Integer Convex Nonlinear Optimization with Gradient-Boosted Trees Embedded* (2018). URL <http://arxiv.org/abs/1803.00952>
- [40] Mitsos, A., Lemonidis, P., Barton, P.I.: Global solution of bilevel programs with a nonconvex inner program. *J. Global Optim.* **42**(4), 475–513 (2008)
- [41] Mockus, J.: On Bayesian methods for seeking the extremum. In: *Proceedings of the IFIP Technical Conference*, pp. 400–404. Springer-Verlag, London, UK, UK (1974)
- [42] Müller, J., Shoemaker, C.A., Piché, R.: SO-MI: A surrogate model algorithm for computationally expensive nonlinear mixed-integer black-box global optimization problems. *Computers and Operations Research* **40**(5), 1383–1400 (2013)
- [43] Nemirovski, A.: On safe tractable approximations of chance constraints. *European Journal of Operational Research* **219**(3), 707–718 (2012)
- [44] Nemirovski, A., Shapiro, A.: Convex approximations of chance constrained programs. *SIAM Journal on Optimization* **17**(4), 959–996 (2006)
- [45] Nemirovski, A., Shapiro, A.: Scenario Approximations of Chance Constraints. *Probabilistic and Randomized Methods for Design under Uncertainty* (2), 3–47 (2006)

- [46] Pagnoncelli, B.K., Ahmed, S., Shapiro, A.: Sample average approximation method for chance constrained programming: Theory and applications. *Journal of Optimization Theory and Applications* **142**(2), 399–416 (2009)
- [47] Picheny, V., Gramacy, R.B., Wild, S., Le Digabel, S.: Bayesian optimization under mixed constraints with a slack-variable augmented Lagrangian. In: *NIPS* (2016)
- [48] Pintér, J.: Deterministic approximations of probability inequalities. *ZOR Zeitschrift für Operations Research Methods and Models of Operations Research* **33**(4), 219–239 (1989)
- [49] Rasmussen, C.E., Williams, C.K.I.: *Gaussian processes for machine learning*. The MIT Press, Cambridge, Massachusetts (2006)
- [50] Regis, R.G., Shoemaker, C.A.: Constrained global optimization of expensive black box functions using radial basis functions. *Journal of Global Optimization* **31**(1), 153–171 (2005)
- [51] Sahinidis, N.V.: Optimization under uncertainty: State-of-the-art and opportunities. *Computers and Chemical Engineering* **28**(6-7), 971–983 (2004)
- [52] Schilling, G., Pantelides, C.C.: A Simple Continuous-Time Process Scheduling Formulation and a Novel Solution Algorithm. *Computers and Chemical Engineering* **20**(96), 1221–1226 (1996)
- [53] Shahriari, B., Swersky, K., Wang, Z., Adams, R.P., De Freitas, N.: Taking the human out of the loop: A review of Bayesian optimization. *Proceedings of the IEEE* **104**(1), 148–175 (2016)
- [54] Snelson, E., Rasmussen, C.E., Ghahramani, Z.: Warped Gaussian processes. In: *NIPS* (2003)
- [55] Snoek, J., Larochelle, H., Adams, R.P.: Practical Bayesian optimization of machine learning algorithms. In: *NIPS*, pp. 2951–2959. USA (2012)
- [56] Soyster, A.L.: Technical Note Convex Programming with Set-Inclusive Constraints and Applications to Inexact Linear Programming. *Oper. Res.* **21**(5), 1154–1157 (1973)

- [57] Ulmasov, D., Baroukh, C., Chachuat, B., Deisenroth, M.P., Misener, R.: Bayesian optimization with dimension scheduling: Application to biological systems. In: Z. Kravanja, M. Bogataj (eds.) 26th European Symposium on Computer Aided Process Engineering, *Computer Aided Chemical Engineering*, vol. 38, pp. 1051 – 1056. Elsevier (2016)
- [58] Varakantham, P., Fu, N., Lau, H.C.: A proactive sampling approach to project scheduling under uncertainty. In: AAAI (2016)
- [59] Wächter, A., Biegler, L.T.: On the implementation of an interior-point filter line-search algorithm for large-scale nonlinear programming. *Math. Program.* **106**(1), 25–57 (2006)
- [60] Wiebe, J., Cecilio, I., Misener, R.: Data-Driven Optimization of Processes with Degrading Equipment. *Industrial & Engineering Chemistry Research* **57**(50), 17177–17191 (2018)
- [61] Williams, C.K.I., Rasmussen, C.E.: Gaussian processes for regression & classification. In: NIPS, pp. 514–520 (2008)
- [62] Xie, W., Ahmed, S.: Distributionally Robust Chance Constrained Optimal Power Flow with Renewables: A Conic Reformulation. *IEEE Transactions on Power Systems* **33**(2), 1860–1867 (2018)

A Table of notation

\tilde{a}_i	uncertain parameter
$F_n^{1-\alpha}$	CDF of the χ^2
u	dual variable
\mathbf{x}, \mathbf{y}	decision variable vectors
\mathbf{y}_i	subset of decision variables \mathbf{y}
\mathbf{z}	observation vector in original space
$f(\cdot)$	black-box objective function
$g(\cdot)$	black-box constraint
$h(\cdot)$	warping function
$K(\cdot, \cdot)$	kernel function of GP
$w(\cdot)$	constraint defining \mathcal{U}
\mathcal{E}^α	α -confidence ellipsoid
\mathcal{U}	(warped) uncertainty set
\mathcal{X}	deterministic feasible set
α	probability of constraint violation
$\boldsymbol{\delta}$	disturbances vector
ϵ	estimated feasibility
ϵ_0	target feasibility
ξ	observation vector in latent space
$\boldsymbol{\psi} = \{a_j, b_j, c_j\}$	parameters of warping function
$\boldsymbol{\mu}$	mean of GP at \mathbf{y}_i
σ_{ij}^2	ij -element of covariance matrix
Σ	covariance matrix of GP at \mathbf{y}_i
<i>Production planning</i>	
c_t	production cost in period t
\tilde{p}_t	uncertain price in period t
x_t	production amount in period t
<i>Drill scheduling</i>	
W	weight on bit
\dot{N}	rotational speed
V	rate of penetration
Δp	differential pressure
R	degradation indicator
M	set of maintenance depths

B Connection to uncertain functions

Consider the following robust optimization problem:

$$\min_{(\mathbf{x}, \mathbf{y}) \in \mathcal{X}} f(\mathbf{x}, \mathbf{y}) \quad (25a)$$

$$\text{s.t.} \quad \sum_{i=1}^n \tilde{g}(\mathbf{y}_i) x_i \leq b \quad \forall \tilde{g} \in \mathcal{U}^g \quad (25b)$$

$$\mathbf{y}_i \in \mathbb{R}^k, k \leq n. \quad (25c)$$

Instead of uncertain parameters, Problem (25) considers an uncertainty set \mathcal{U}^g over uncertain functions $\tilde{g}(\cdot)$. We are interested in defining \mathcal{U}^g in a way that it contains “likely” realizations of the GP.

Recall that for any finite set of points $\mathbf{y}_1, \dots, \mathbf{y}_l, l \in \mathbb{N}$:

$$G_{\mathbf{y}_1, \dots, \mathbf{y}_l} = [G(\mathbf{x}_1), \dots, G(\mathbf{x}_l)]^\top \quad (26)$$

is a multivariate Gaussian with mean $\boldsymbol{\mu}(\mathbf{y}_1, \dots, \mathbf{y}_l)$ and covariance $\Sigma(\mathbf{y}_1, \dots, \mathbf{y}_l)$. For any such $G_{\mathbf{y}_1, \dots, \mathbf{y}_l}$, we can construct a confidence ellipsoid $\mathcal{E}^\alpha(\mathbf{y}_1, \dots, \mathbf{y}_l)$ containing the true values $[g(\mathbf{x}_1), \dots, g(\mathbf{x}_l)]^\top$ with probability $1 - \alpha$:

$$\mathcal{E}^\alpha(\mathbf{y}_1, \dots, \mathbf{y}_l)_l = \left\{ \begin{array}{l} \mathbf{z} \in \mathbb{R}^l \\ \text{s.t. } (h(\mathbf{z}) - \boldsymbol{\mu})^\top \Sigma^{-1} (h(\mathbf{z}) - \boldsymbol{\mu}) \\ \leq F_l^{1-\alpha} \end{array} \right\},$$

where $F_l^{1-\alpha} = F_l(1 - \alpha)$ is the cumulative distribution function of the χ^2 distribution with l degrees of freedom. We then construct a set \mathcal{U}^g over functions $\tilde{g}(\cdot)$ for which $[\tilde{g}(\mathbf{x}_1), \dots, \tilde{g}(\mathbf{x}_l)]$ lies in the corresponding α -confidence ellipsoid $\mathcal{E}^\alpha(\mathbf{y}_1, \dots, \mathbf{y}_l)_l$ for any $l \in \mathbb{N}$ and $\mathbf{y}_1, \dots, \mathbf{y}_l$ with $\mathbf{x}_i \in \mathbb{R}^k$:

$$\mathcal{U}^\mathcal{E} = \left\{ \begin{array}{l} \tilde{g} : \mathbb{R}^k \rightarrow \mathbb{R} \text{ s.t.} \\ [\tilde{g}(\mathbf{x}_1), \dots, \tilde{g}(\mathbf{x}_l)]^\top \in \mathcal{E}^\alpha(\mathbf{y}_1, \dots, \mathbf{y}_l), \\ \forall \{\mathbf{y}_1, \dots, \mathbf{y}_l\}, \mathbf{y}_i \in \mathbb{R}^k, l \in \mathbb{N} \end{array} \right\}$$

Replacing \mathcal{U}^g with $\mathcal{U}^\mathcal{E}$ transforms Problem (25) into a robust optimization problem with an uncertainty set over functions defined by an infinite number of confidence ellipsoids which can have arbitrarily many dimensions. This set is not semialgebraic and it is not clear how it could practically be used in optimization. In practice, however, we are only interested in evaluating the GP at a finite number of points.

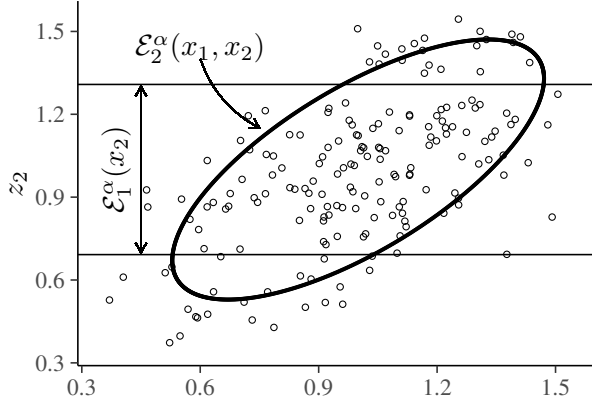


Figure 12: Any l_1 -dimensional α -confidence ellipsoid $\mathcal{E}_{l_1}^\alpha$ is a strict subset of the projection of higher order α -confidence ellipsoids $\mathcal{E}_{l_2}^\alpha$, $l_2 > l_1$ onto the l_1 -dimensional space.

Here, the number of evaluation points is the number of times $|S|$ that the GP occurs in the optimization problem. Consider the following robust optimization problem:

$$\min_{(\mathbf{x}, \mathbf{y}) \in \mathcal{X}} f(\mathbf{x}, \mathbf{y}) \quad (27a)$$

$$\text{s.t. } \mathbf{z}^\top \mathbf{x} \leq b \quad \forall \mathbf{z} \in \mathcal{E}^\alpha(\mathbf{y}) \quad (27b)$$

$$\mathbf{y}_i \in \mathbb{R}^k, k \leq n. \quad (27c)$$

Theorem 1. A vector \mathbf{x}^* which is a feasible solution to Problem (27) is also a feasible solution to Problem (25).

Proof. Assume \mathbf{x}^* is a solution to Problem (27) but not to Problem (25). Then $\exists \hat{g} \in \mathcal{U}^g$ s.t. $\sum_{i \in S} \hat{g}(\mathbf{x}_i^*) x_i^* > 0$. The definition of \mathcal{U}^g implies that $[\hat{g}(\mathbf{x}_i^*) : i \in S]^\top \in \mathcal{E}^\alpha(\mathbf{x}_i^* : i \in S)$. Choosing $\hat{\mathbf{z}} = [\hat{g}(\mathbf{x}_i^*) : i \in S]^\top$, it follows that $\sum_{i \in S} \hat{z}_i x_i^* = \sum_{i \in S} \hat{g}(\mathbf{x}_i^*) x_i^* > 0$, meaning that $\{\mathbf{x}^*, \hat{\mathbf{z}}\}$ is not feasible in Problem (27). But $\hat{\mathbf{z}} \in \mathcal{E}^\alpha(\mathbf{y}_i^* : i \in [n])$, which is a contradiction. \square

Fig. (12) shows that the converse of Theorem (1) is not necessarily true. Because all confidence ellipsoids are symmetric and centered at the mean of the distribution, any lower dimensional ellipsoid $\mathcal{E}_l^\alpha = \mathcal{E}^\alpha(\mathbf{y}_1, \dots, \mathbf{y}_l)$, $l < n$ is a strict subset of the projection of $\mathcal{E}_n^\alpha = \mathcal{E}^\alpha(\mathbf{y})$ onto the l -dimensional space (otherwise it would have to

contain a larger probability mass). Problem (27) therefore conservatively approximates Problem (25). Furthermore, the α -confidence ellipsoid $\mathcal{E}^\alpha(\mathbf{y})$ implies that a solution to Problem (27) is a feasible solution to the black-box constrained problem with a probability of at least $1 - \alpha$ (see Theorem 1).

C Globally optimizing non-convex inner maximization problems

Lemma 6. *Let \mathbf{z}^* be the solution of Problem ??, then $\mathbf{z}^* \in \partial\mathcal{U}$.*

Proof. For the sake of contradiction assume $\mathbf{z}^* \in \text{int}(\mathcal{U})$, then $\exists \epsilon > 0$ s.t. $\mathbf{z}_0 \in \mathcal{U} \forall \mathbf{z}_0 \in \{\mathbf{z}_0 \mid \|\mathbf{z}^* - \mathbf{z}_0\| < \epsilon\}$. Let:

$$\hat{\mathbf{z}} = \mathbf{z}^* + \frac{\mathbf{x}}{\|\mathbf{x}\|} \frac{\epsilon}{2},$$

then:

$$\|\mathbf{z}^* - \hat{\mathbf{z}}\| = \|\mathbf{z}^* - \mathbf{z}^* - \frac{\mathbf{x}}{\|\mathbf{x}\|} \frac{\epsilon}{2}\| = \frac{\epsilon}{2} < \epsilon,$$

and therefore $\hat{\mathbf{z}} \in \mathcal{U}$, but:

$$\mathbf{x}^\top \hat{\mathbf{z}} = \mathbf{x}^\top \left(\mathbf{z}^* - \frac{\mathbf{x}}{\|\mathbf{x}\|} \frac{\epsilon}{2} \right) = \mathbf{x}^\top \mathbf{z}^* + \frac{\mathbf{x}^\top \mathbf{x}}{\|\mathbf{x}\|} \frac{\epsilon}{2} > \mathbf{x}^\top \mathbf{z}^*,$$

which is a contradiction. □

Lemma 7. *The bounding box of an ellipsoid $\mathbf{x}^\top \Sigma^{-1} \mathbf{x}$ is given by the extreme points $x_i = \pm r \sigma_{ii}$*

Proof. Consider the optimization problem:

$$\max_{\mathbf{x}} x_i \tag{28a}$$

$$\text{s.t. } \mathbf{x}^\top \Sigma^{-1} \mathbf{x} = r^2 \tag{28b}$$

It's stationarity condition is:

$$\boldsymbol{\delta} = 2\lambda \Sigma^{-1} \mathbf{x} \tag{29}$$

Pre-multiplying by \mathbf{x}^\top and substituting primal feasibility leads to the expression:

$$\lambda = \frac{x_i}{2r^2}. \tag{30}$$

Substituting this back into the stationarity condition and rearranging gives:

$$\mathbf{x} = \frac{r^2}{x_i} \Sigma \delta, \quad (31)$$

which, substituted into the primal constraint leads to the desired results:

$$x_i = \pm r \sigma_{ii} \quad (32)$$

□

D Drill scheduling model

In order to connect the penetration rate V and degradation rate r to the drilling parameters, weight-on-bit W and rotational speed \dot{N} , we require two models:

- A *bit-rock interaction model* [22] connecting W and \dot{N} with V and differential pressure across the mud motor Δp
- A *mud motor degradation model* [2] connecting the degradation rate r with the differential pressure Δp .

D.1 Detournay's bit-rock interaction model

To model the connection between W , \dot{N} , V , and Δp , we combine the bit-rock interaction model by Detournay et al. [22] with the PDM's powercurve. There are three relevant rotational speeds in the drilling process: The drill-string speed \dot{N}_{top} , the PDM speed (relative to the drill string) \dot{N}_{PDM} , and the drill-bit speed \dot{N}_{bit} :

$$\dot{N}_{bit} = \dot{N}_{top} + \dot{N}_{PDM} \quad (33)$$

Based on Detournay et al. [22], the following drilling response model can be formulated relating N_{bit} with the weight-on-bit W and the rate of penetration V :

$$V = d \cdot \dot{N}_{bit} \quad [22, \text{Eq. 4}] \quad (34a)$$

$$w = \frac{W}{a(1 - \rho)} \quad [22, \text{Eq. 4}] \quad (34b)$$

$$d = \begin{cases} \frac{w}{S^*} \\ \frac{w^*}{S^*} + \frac{w-w^*}{\xi \epsilon} \end{cases} \quad [22, \text{Eqs. 24,37}] \quad (34c)$$

$$(34d)$$

where d is the depth of cut per revolution, w is a scaled weight-on-bit, and a , ρ , S^* , w^* , $\xi\epsilon$, N^{max} , and W^{max} are rock and equipment parameters.

The relationship between torque T and weight-on-bit W is given by:

$$t = \frac{2T}{a^2(1 - \rho^2)} \quad [22, \text{Eqn. 4}]$$

$$t = \begin{cases} \mu\gamma'w \\ \frac{1}{\xi}(w - (1 - \beta)w^*) \end{cases} \quad [22, \text{Eqns. 29,38}] \quad (35)$$

For the bit parameters $a = 100.4$ and $\rho = 0.0$ was used. Rock parameters are available for Lower Jurassic shale and Sandstone in the open literature[22]:

Parameter	Lower Jurassic shale	Sandstone
S^* [MPa]	278	315
w^* [N/mm]	199	59
$\xi\epsilon$ [MPa]	125	50
$\mu\gamma'$ [-]	0.48	0.93
$(1 - \beta)w_{f*}$ [N/mm]	157	33
ξ [-]	0.98	0.65

Using the PDM's power curve (Fig. 13), the bit rotational speed \dot{N}_{bit} can be determined as a function of \dot{N} , T , and Δp . Fig. 13 shows the relationship between T , \dot{N}_{PDM} , the differential pressure over the PDM Δp , and the flow rate through the PDM \dot{Q} . Since torque T is specified through W (Eqn. 35), Δp can be determined from the power curve (Fig. 13). If additionally the flow $\dot{Q}(t)$ is given, \dot{N}_{PDM} is also fully specified.

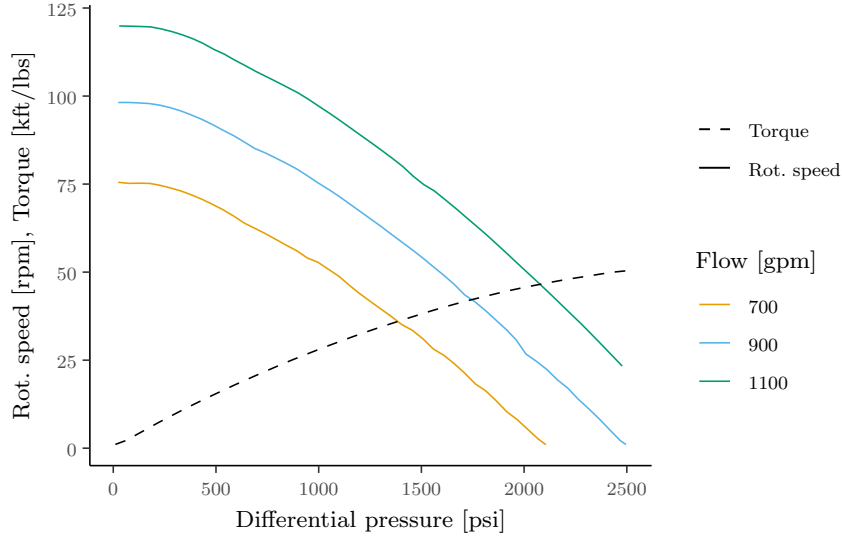


Figure 13: Example of a PDM power curve. [2]

Putting this together, we obtain the following model relating V to W and \dot{N} :

$$V = d \left(\dot{N}_{top} + \dot{N}_{PDM} \right) \quad (36a)$$

$$w = \frac{W}{a(1 - \rho)} \quad (36b)$$

$$t = \frac{2T}{a^2(1 - \rho^2)} \quad (36c)$$

$$t = \begin{cases} \mu\gamma'w \\ \frac{1}{\xi}(w - (1 - \beta)w^*) \end{cases} \quad (36d)$$

$$d = \begin{cases} \frac{w}{S^*} \\ \frac{w^*}{S^*} + \frac{w-w^*}{\xi\epsilon} \end{cases} \quad (36e)$$

$$\dot{N}_{PDM} = f \left(T, \dot{Q} \right) \quad (\text{from Fig. 13}) \quad (36f)$$

$$\dot{N}_{top} \leq \dot{N}^{max} \quad (36g)$$

$$W \leq W^{max} \quad (36h)$$

$$(\text{safety constraints}), \quad (36i)$$

Assuming that the flow rate $\dot{Q}(t)$ is treated as a parameter, the only decision variables are $W(t)$, and $\dot{N}_{top}(t)$. For the purpose of this work we model the above power

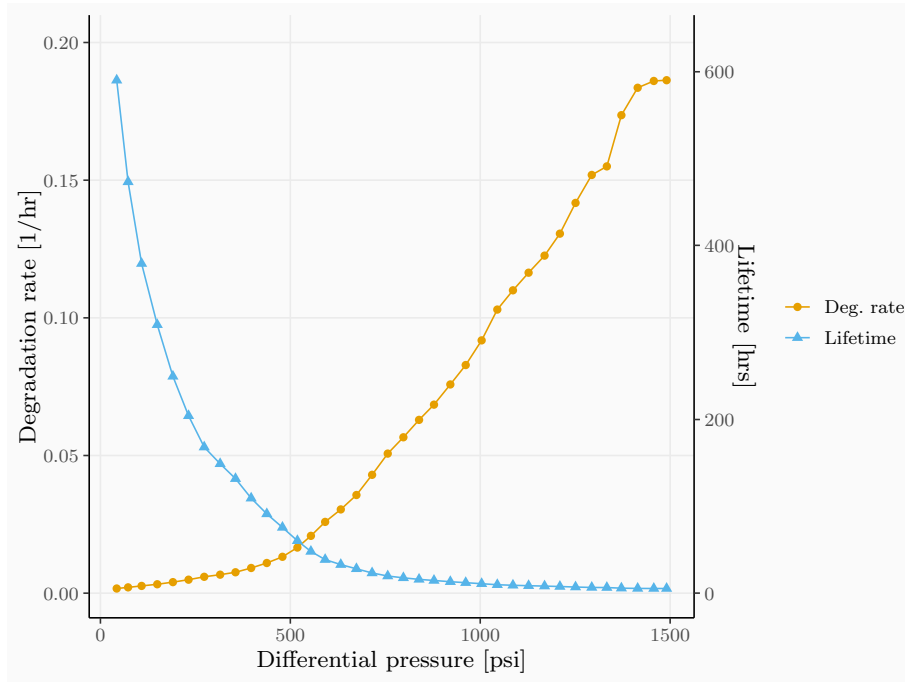


Figure 14: Maximum lifetime of a PDM as a function of differential Δp (for a given PDM geometry and elastomer, mud, flow, and temperature).[2]

curves using quadratic equations. Notice that the variables w, t, d , and \dot{N}_{PDM} could easily be eliminated, resulting in a more compact albeit less intuitive/physically meaningful formulation.

D.2 Mud motor degradation model

For the mud motor degradation characteristics we use data obtained by Ba et al. [2], determined through a combination of simulation and experiments, shown in Fig. 14. [2].